Journal of Gastroenterology and Hepatology JGHF

doi:10.1111/j.1440-1746.2011.06988.x

EDUCATION AND IMAGING

Hepatobiliary and Pancreatic: Detection of early hepatocellular carcinoma by enhanced magnetic resonance imaging

A woman, aged 75, with cirrhosis caused by hepatitis C had a routine ultrasound study for surveillance for hepatocellular carcinoma. A possible nodule was identified in segment VI but it was difficult to identify the contours or margins of the nodule. A contrast-enhanced ultrasound (US) study with perfluorobutane (Sonazoid®) showed no enhancement or washout of the nodule in either the vascular or Kupffer phases. Computed tomography (CT) during hepatic arteriography (CTHA) or arterial portography (CTAP) also failed to show a liver lesion (Figure 1, left and middle panel). In contrast, gadolinium ethoxybenzyl diethylenetriamine pentaacetic acid (Primovist®)-enhanced magnetic resonance imaging (MRI) clearly revealed a low-signal nodule during the hepatobiliary phase (Figure 1, right). The appearance was consistent with either a dysplastic nodule or a well-differentiated hepatocellular carcinoma. As the nodule could not be detected on US or CT, we performed real-time virtual sonography synchronizing B-mode US images with the hepatobiliary phase of enhanced MRI which allowed for the same area to be displayed in real time as both MR and B-mode US images (Figure 2). Using this technique, the nodule was clearly visualized and an aspiration biopsy was performed. Histology revealed a well-to-moderately differentiated hepatocellular carcinoma that was treated by percutaneous radiofrequency ablation guided by real-time virtual sonography with contrast-enhanced MRI.

Radiofrequency ablation is widely used for the treatment of hepatocellular carcinoma. However, to achieve successful ablation, it is important to have a clear view of the margins of the nodule. Although most larger hepatocellular carcinomas are hypervascular, early carcinomas can be hypovascular and can be difficult to detect with contrast-enhanced US, contrast-enhanced CT or CT during hepatic arteriography. The recent introduction of contrast-enhanced MRI appears to have improved the detection of early liver tumors and may be helpful for the differentiation of early hepatocellular carcinoma from dysplastic nodules. Real-time virtual sonography is a system in which a B-mode US image can be synchronized with CT images. To our knowledge, this is the first report of the successful use of real-time virtual sonography with enhanced MRI for the detection and treatment of an early hepatocellular carcinoma. This technology may facilitate the diagnosis and treatment of hepatocellular carcinoma at an earlier stage.

Contributed by
Y Eso*, H Marusawa* & Y Osaki†
**Department of Gastroenterology and Hepatology, Graduate School of Medicine, Kyoto University, Kyoto and †Department of Gastroenterology and Hepatology, Osaka Red Cross Hospital, Osaka, Japan*

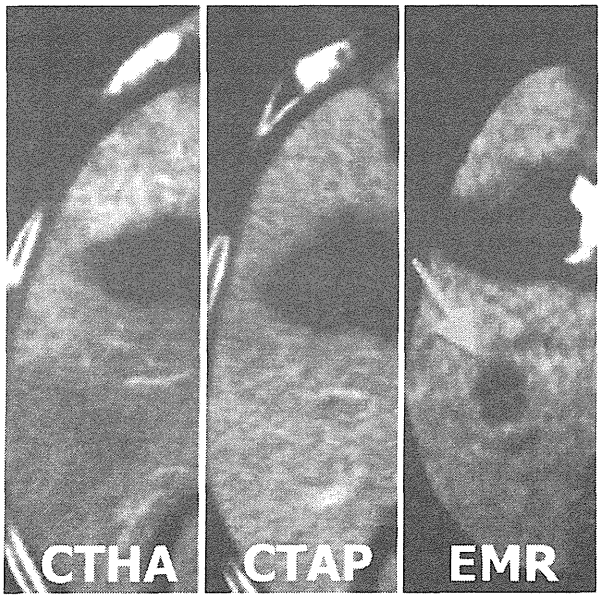

Figure 1

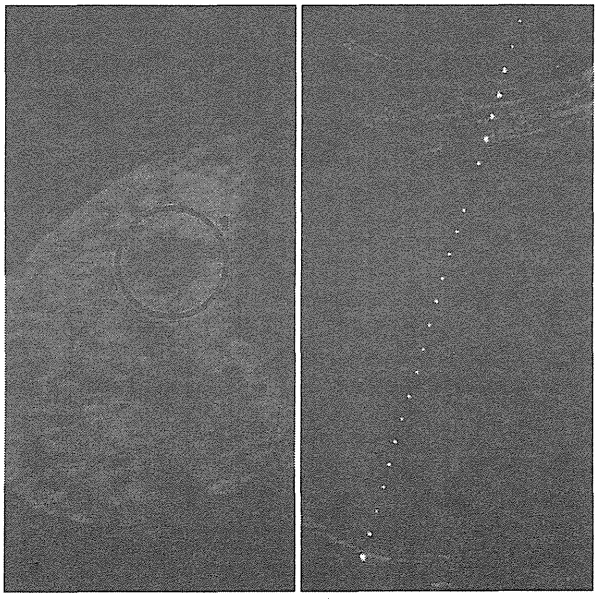

Figure 2

ANNALS of Hepatology

LETTER TO EDITOR

July-August, Vol. 11 No.4, 2012: 572-573

Idiopathic portal hypertension with multiple hepatic hyperplastic nodules supplied by portal vein

Atsuyuki Ikeda,*,** Ryuichi Kita,* Akihiro Nasu,*,** Norihiro Nishijima,*,**
Hiroo Matsuo,* Toru Kimura,* Yukio Osaki,* Makoto Ohbu***

* Department of Gastroenterology and Hepatology, Osaka Red Cross Hospital, Fudegasaki-cho, Tennoji-ku, Osaka, Japan.
** Department of Gastroenterology and Hepatology, Kyoto University Graduate School of Medicine, Shogoin-Kawaracho 54, Sakyo-ku, Kyoto, Japan.
*** Department of Pathology, Kitasato University School of Allied Health Sciences, Sagamihara, Kanagawa, Japan.

Dear Editor

Hepatic nodules with increased portal venous flow are rare, and no distinct status has been established for them. We present here a case of idiopathic portal hypertension (IPH) with multiple hyperplastic nodules supplied by portal venous flow.

A 30-year-old Japanese man with esophageal varices was admitted to our hospital. Arterial phase computed tomography (CT) revealed multiple low-attenuating nodules of 2 to 3 cm in diameter in both lobes. However the contrast of the multiple nodules had become indistinct on portal phase CT. Multiple nodules showed strongly high-attenuation on CT during arterial portography (CTAP) (Figure 1A) and low-attenuation on CT during hepatic arteriography. Single-level dynamic CTAP (S-CTAP) was also performed as described previously[1] (Figure 1B-1E). Regions of interest (ROIs) were placed on the images of the nodules and adjacent liver parenchyma, and their density was measured and plotted to construct a time-density curve. S-CTAP clearly

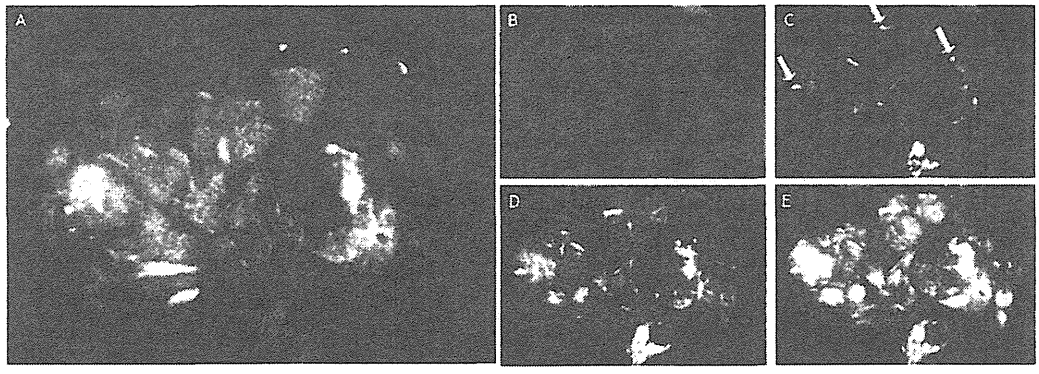

Figure 1. Single-level dynamic computed tomography during arterial portography (CTAP) and histopathology of the nodules. Multiple nodules showed strong high-attenuation on CTAP (A). The nodules were a few centimeters in diameter and distributed throughout the liver. Single-level dynamic CTAP images were obtained at 6 s (B), 14 s (C), 18 s (D), and 22 s (E) after injection of contrast material from the superior mesenteric artery. Within 14 s (C), the feeding vessels and partial enhancement in the nodules had become visible (arrows). The contour of the nodules became evident in 18 s (D), and the entire nodule became highly enhanced in 22 s (E).

Correspondence and reprint request: Ryuichi Kita, M.D., Ph.D.
Department of Gastroenterology and Hepatology, Osaka Red Cross Hospital. 5-53 Fudegasaki-cho, Tennoji-ku, Osaka 543-8555.
Telephone: +81-6-6774-5111. Fax: +81-6-6774-5131.
E-mail: r-kita@osaka-med.jrc.or.jp

Manuscript received:November 24, 2011.
Manuscript accepted: December 14,2011.

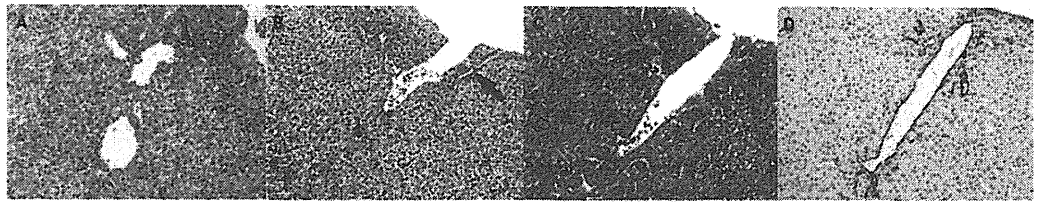

Figure 2. Liver biopsy specimens taken from the nodular regions showed neither cellular nor structural atypia, but did reveal liver cell hyperplasia (A-C). There were many dilated thin-walled vessels without coexistence of arteries or bile ducts. Some of them were accompanying only bile duct (B) (arrow). Some dilated vessels distributing into lobules were observed in serial sections (B-D). CD34 immunostaining showed the existence of endothelial cells on the lumens of this dilated vessels and that these were not dilated sinusoids. [H&E staining (A); Reticulin Silver impregnation staining (B); Azan Mallory staining (C); CD34 immunostaining (D)].

showed the contrast material in the small portal branches in the nodules, which spread throughout the entire nodule. The peak value of the time-density curve was 246 HU for the ROIs placed on the nodule, which was extremely high in comparison with the value on a normal parenchyma. Histologically, the nodules showed neither cellular nor structural atypia, but showed liver cell hyperplasia. Inside the nodule, dilated venous-like vessels were observed (Figure 2A). Most of them were seen to distribute in lobules without coexistence of artery or bile duct, but some were with only bile ductile by investigation of serial thin sections (Figure 2B-2D). These findings indicated that they originated from the portal vein.[2]

There are two possible reasons for hyper-attenuation on CTAP; one is that portal blood flow to the nodule increases absolutely, and the other is that portal blood flow to the nodule increases relative to the surrounding parenchyma adjacent to the nodule.[3] In this case, S-CTAP and the time-density curve clearly indicated that portal venous flow to these nodules showed an absolute increase. It was also supported by the presence of dilated vessels within the nodules. These indicated that increased portal venous flow was distributed into the hyperplastic nodules by the dilated vessels originated from portal vein. In summary, we reported a case of IPH with multiple hepatic hyperplastic nodules supplied by the portal venous flow. S-CTAP and the time-density curve were very useful to confirm the portal venous flow.

STATEMENT OF CONFLICTS OF INTEREST

I have none declared.

REFERENCES

1. Miyayama S, Matsui O, Zen Y, et al. Focal hepatic lesions mimicking cavernous hemangioma supplied by the portal vein. *Hepatol Res* 2006; 36: 70-3.
2. Ohbu M, Okudaira M, Watanabe K, et al. Histopathological study of intrahepatic aberrant vessels in cases of noncirrhotic portal hypertension. *Hepatology* 1994; 20: 302-8.
3. Onaya H, Itai Y, Satake M, et al. Highly enhanced hepatic masses seen on CT during arterial portography: early hepatocellular carcinoma and adenomatous hyperplasia. *Jpn J Clin Oncol* 2000; 30: 440-5.

Endoscopic ultrasonography-guided transgastric drainage of infectious biloma following radiofrequency ablation for hepatocellular carcinoma

Journal:	*Digestive Endoscopy*
Manuscript ID:	JGES-DEN-2012-2894.R1
Manuscript Type:	Letters, techniques and images
Date Submitted by the Author:	13-Feb-2012
Complete List of Authors:	Eso, Yuji; Kyoto University Graduate School of Medicine, Gastroenterology and Hepatology Marusawa, Hiroyuki; Kyoto University Graduate School of Medicine, Gastroenterology and Hepatology Tsumura, Takehiko; Osaka Red Cross Hospital, Gastroenterology and Hepatology Okabe, Yoshihiro; Osaka Red Cross Hospital, Gastroenterology and Hepatology Osaki, Yukio; Osaka Red Cross Hospital, Gastroenterology and Hepatology
Keyword - Please refer to MESH keyword list. (See above for URL):	Endosonography, Liver Abscess, drainage, Carcinoma, Hepatocellular
Please choose 1 to 5 categories from the list provided that describes your manuscript. This will aid in finding suitable reviewers for your manuscript.:	Biliary / Pancreatic: EUS, Biliary / Pancreatic: Biliary tract, Stomach: Endoscopic treatment

<Title>

Endoscopic ultrasonography-guided transgastric drainage of infectious biloma following radiofrequency ablation for hepatocellular carcinoma

<Author>

YUJI ESO,[1] HIROYUKI MARUSAWA,[1] TAKEHIKO TSUMURA,[2] YOSHIHIRO OKABE[2] AND YUKIO OSAKI[2]

[1]*Department of Gastroenterology and Hepatology, Graduate School of Medicine, Kyoto University, Kyoto, Japan; and* [2]*Department of Gastroenterology and Hepatology, Osaka Red Cross Hospital, Osaka, Japan*

Corresponding author: Hiroyuki Marusawa, M.D., and Ph.D.

Department of Gastroenterology and Hepatology

Kyoto University Graduate School of Medicine, Kyoto, Japan

Shogoin-Kawaracho 54, Sakyo-ku, Kyoto, 606-8507, Japan

Phone; +81-75-751-4319

Fax; +81-75-751-4303

E-mail; maru@kuhp.kyoto-u.ac.jp

(We do not need offprints.)

Conflicts of interest:

The authors disclose no conflicts.

<Text>

An 87-year-old female was diagnosed with a 22-mm diameter hepatocellular carcinoma in segment II and treated by percutaneous ultrasound-guided radiofrequency ablation (RFA). Six months later, she presented to the emergency room complaining of high fever and general malaise. Computed tomography images showed a 96×60-mm fluid collection in the left lobe of the liver (Fig. 1). She was diagnosed with sepsis due to biloma infection caused by RFA-mediated bile duct disruption. Because the biloma was adjacent to the stomach, we performed endoscopic ultrasonography (EUS)-guided transgastric drainage of the biloma. A discharge of pus was observed following the creation of internal and external fistulas between the biloma and stomach using 7F double-pigtail stent and 7.5F single-pigtail tube (Fig. 2) and cultures of the purulent fluid grew *Escherichia coli*. A computed tomography scan obtained 4 weeks after drainage confirmed complete resolution of the biloma and the patient recovered uneventfully.

Although biloma formation related to bile duct disruption is a frequent complication of RFA, biloma infection complicated with bacteremia is very rare.[1] Bilomas are usually treated by either percutaneous drainage or surgery. This patient, however, was very elderly and had advanced dementia, so it was difficult for her to keep still during percutaneous puncture. In addition, the risk for self-removal of drainage tube was also considered to be high. The utility of EUS-guided drainage of intra-abdominal fluid collections is well documented,[2] whereas there have been a small number of reports on EUS-guided drainage of bilomas.[3] The biloma in this patient was located adjacent to the stomach; therefore, EUS-guided drainage was considered to be a promising alternative and was successfully performed. In summary, the risk of biloma infection should be considered, especially in putative immune-compromised older patients. Moreover, careful attention must be paid to the possibility of delayed biloma infection even 6 months after RFA.

<REFERENCES>

1. Chang I, Rhim H, Kim S *et al.* Biloma formation after radiofrequency ablation of hepatocellular carcinoma: incidence, imaging features, and clinical significance. *Am J Roentgenol.* 2010; **195**: 1131-1136.

2. Piraka C, Shah R, Fukami N *et al.* EUS-guided transesophageal, transgastric, and transcolonic drainage of intra-abdominal collections and abscesses. *Gastrointest. Endosc.* 2009; **70**:786-792.

3. Shami VM, Talreja JP, Mahajan A *et al.* EUS-guided drainage of bilomas: a new alternative? *Gastrointest. Endosc.* 2008; **67**:136-140.

<Figure legends>

Fig. 1. CT findings of a 96×60-mm fluid collection in the left lobe of the liver, suggestive for infectious biloma.

Fig. 2. Endoscopic findings of the discharge of pus following the creation of fistulas between the biloma and stomach using 7F double-pigtail stent and 7.5F single-pigtail tube.

<Title>

Endoscopic ultrasonography-guided transgastric drainage of infectious biloma following radiofrequency ablation for hepatocellular carcinoma

<Author>

YUJI ESO,[1] HIROYUKI MARUSAWA,[1] TAKEHIKO TSUMURA,[2] YOSHIHIRO OKABE[2] AND YUKIO OSAKI[2]

[1]*Department of Gastroenterology and Hepatology, Graduate School of Medicine, Kyoto University, Kyoto, Japan; and* [2]*Department of Gastroenterology and Hepatology, Osaka Red Cross Hospital, Osaka, Japan*

Corresponding author: Hiroyuki Marusawa, M.D., and Ph.D.

Department of Gastroenterology and Hepatology

Kyoto University Graduate School of Medicine, Kyoto, Japan

Shogoin-Kawaracho 54, Sakyo-ku, Kyoto, 606-8507, Japan

Phone; +81-75-751-4319

Fax; +81-75-751-4303

E-mail; maru@kuhp.kyoto-u.ac.jp

(We do not need offprints.)

Conflicts of interest:

The authors disclose no conflicts.

<Text>

An 87-year-old female was diagnosed with a 22-mm diameter hepatocellular carcinoma in segment II and treated by percutaneous ultrasound-guided radiofrequency ablation (RFA). Six months later, she presented to the emergency room complaining of high fever and general malaise. Computed tomography images showed a 96×60-mm fluid collection in the left lobe of the liver (Fig. 1). She was diagnosed with sepsis due to biloma infection caused by RFA-mediated bile duct disruption. Because the biloma was adjacent to the stomach, we performed endoscopic ultrasonography (EUS)-guided transgastric drainage of the biloma. A discharge of pus was observed following the creation of internal and external fistulas between the biloma and stomach using 7F double-pigtail stent and 7.5F single-pigtail tube (Fig. 2) and cultures of the purulent fluid grew *Escherichia coli*. A computed tomography scan obtained 4 weeks after drainage confirmed complete resolution of the biloma and the patient recovered uneventfully.

Although biloma formation related to bile duct disruption is a frequent complication of RFA, biloma infection complicated with bacteremia is very rare.[1] Bilomas are usually treated by either percutaneous drainage or surgery. This patient, however, was very elderly and had advanced dementia, so it was difficult for her to keep still during percutaneous puncture. In addition, the risk for self-removal of drainage tube was also considered to be high. The utility of EUS-guided drainage of intra-abdominal fluid collections is well documented,[2] whereas there have been a small number of reports on EUS-guided drainage of bilomas.[3] The biloma in this patient was located adjacent to the stomach; therefore, EUS-guided drainage was considered to be a promising alternative and was successfully performed. In summary, the risk of biloma infection should be considered, especially in putative immune-compromised older patients. Moreover, careful attention must be paid to the possibility of delayed biloma infection even 6 months after RFA.

<REFERENCES>

1. Chang I, Rhim H, Kim S *et al.* Biloma formation after radiofrequency ablation of hepatocellular carcinoma: incidence, imaging features, and clinical significance. *Am J Roentgenol.* 2010; **195**: 1131-1136.

2. Piraka C, Shah R, Fukami N *et al.* EUS-guided transesophageal, transgastric, and transcolonic drainage of intra-abdominal collections and abscesses. *Gastrointest. Endosc.* 2009; **70**:786-792.

3. Shami VM, Talreja JP, Mahajan A *et al.* EUS-guided drainage of bilomas: a new alternative? *Gastrointest. Endosc.* 2008; **67**:136-140.

<Figure legends>

Fig. 1. CT findings of a 96×60-mm fluid collection in the left lobe of the liver, suggestive for infectious biloma.

Fig. 2. Endoscopic findings of the discharge of pus following the creation of fistulas between the biloma and stomach using 7F double-pigtail stent and 7.5F single-pigtail tube.

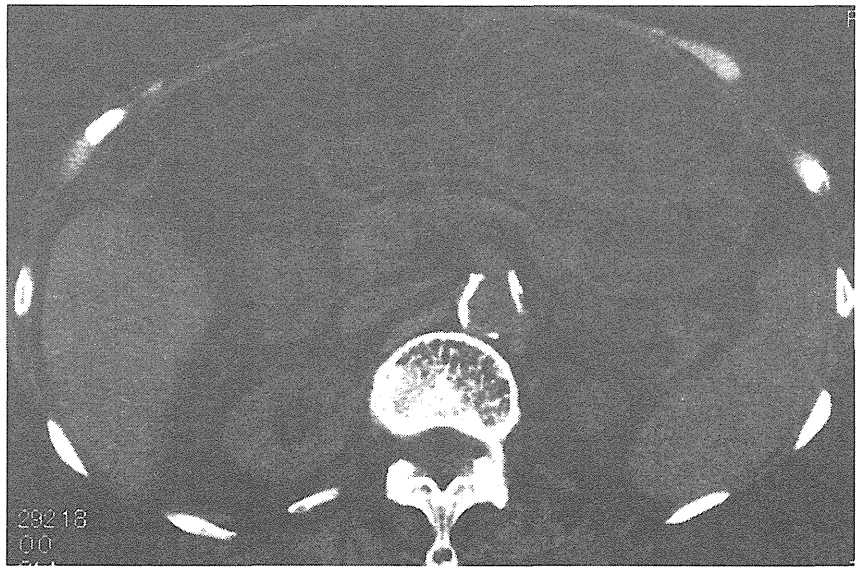

Figure 1
CT findings of a 96×60-mm fluid collection in the left lobe of the liver, suggestive for infectious biloma.
119x78mm (99 x 99 DPI)

Figure 2
Endoscopic findings of the discharge of pus following the creation of a fistula between the biloma and stomach using a 7F plastic stent.
119x119mm (96 x 96 DPI)

RESPONSE TO REVIEWER:

We wish to express our appreciation to the Reviewer for his or her insightful comments, which have helped us improve the paper.

Comment 1: *Figure 2: The endoscopic image might cause misunderstanding that two stents were placed. The stent must be a 7F double-pigtail type stent.*

Response: We regret that our expression of this information was incorrect. In accordance with the Reviewer's comment, we have changed the following text from (line 7):

"A discharge of pus was observed following the creation of a fistula between the biloma and stomach using a 7F plastic stent (Fig. 2) and cultures of the purulent fluid grew *Escherichia coli.*"

to

"A discharge of pus was observed following the creation of internal and external fistulas between the biloma and stomach using 7F double-pigtail stent and 7.5F single-pigtail tube (Fig. 2) and cultures of the purulent fluid grew *Escherichia coli.* "

Further, we have changed the figure legend from:

"Fig. 2. Endoscopic findings of the discharge of pus following the creation of a fistula between the biloma and stomach using a 7F plastic stent."

to

"Fig. 2. Endoscopic findings of the discharge of pus following the creation of fistulas between the biloma and stomach using 7F double-pigtail stent and 7.5F single-pigtail tube."

Comment 2: *EUS-guided drainage of biloma was previously reported by Shami VM et al. (Gastrointest Endosc 2008:67(1):136-40). This article should be referred.*

Response: In accordance with the Reviewer's comment, we have changed the following text from (line 16):

"The utility of EUS-guided drainage of intra-abdominal fluid collections and abscesses is well documented.[2] "

to

"The utility of EUS-guided drainage of intra-abdominal fluid collections is well documented,[2] whereas there have been a small number of reports on EUS-guided drainage of bilomas.[3]"

Further, we have also added the following reference.

"3. Shami VM, Talreja JP, Mahajan A *et al.* EUS-guided drainage of bilomas: a new alternative? *Gastrointest. Endosc.* 2008; **67**:136-140."

We wish to thank the Reviewer again for his or her valuable comments.

Cancer Science

Novel method to measure serum levels of des-gamma-carboxy prothrombin for hepatocellular carcinoma in patients taking warfarin: A preliminary report

Hidenori Toyoda,[1,4] Takashi Kumada,[1] Yukio Osaki,[2] Toshifumi Tada,[1] Yuji Kaneoka[3] and Atsuyuki Maeda[3]

[1]Department of Gastroenterology, Ogaki Municipal Hospital, Ogaki, Japan; [2]Department of Gastroenterology, Osaka Red Cross Hospital, Osaka, Japan; [3]Department of Surgery, Ogaki Municipal Hospital, Ogaki, Japan

(Received November 4, 2011/Revised January 30, 2012/Accepted January 31, 2012/Accepted manuscript online February 9, 2012)

Des-gamma-carboxy prothrombin (DCP) is a useful tumor marker for hepatocellular carcinoma (HCC), but its utility is limited in patients taking vitamin K antagonists. We evaluated the NX-DCP ratio, a newly developed method to measure serum DCP, for its ability to identify DCP elevation induced by HCC in this patient subpopulation. Conventional DCP measurements and the NX-DCP ratio were compared in patients with and without HCC, all of whom were taking the vitamin K antagonist warfarin. We found no differences in conventional DCP measurements between patients with and without HCC due to warfarin treatment. In contrast, the NX-DCP ratio was significantly higher in patients with HCC; the NX-DCP ratio in all patients without HCC was <1.50. When the cut-off was fixed at 1.50, sensitivity and specificity for HCC diagnosis were 60.0% and 100.0%, respectively, which are comparable to those of conventional DCP measurements in patients not taking warfarin. The novel NX-DCP ratio identifies patients on warfarin with elevated DCP due to HCC and is useful as a tumor marker for HCC in this patient subpopulation. (*Cancer Sci*, doi: 10.1111/j.1349-7006.2012.02232.x, 2012)

Prothrombin, or coagulation factor II, is a 71 600 Da protein that consists of three regions: fragment 1; fragment 2; and prothrombin. Fragment 1 consists of 156 amino acids, including 41 amino acids forming an *N*-terminal gamma-glutamic acid (Gla)-containing domain. Prothrombin is first synthesized in the liver as a precursor with 10 glutamic acid (Glu) residues, which are then modified to Gla residues by gamma-glutamylcarboxylase in the presence of vitamin K, O_2, and CO_2 before it is released into the bloodstream.

However, in the absence of vitamin K or in the presence of vitamin K antagonists, gamma-carboxylation is impaired, and prothrombin with the remaining Glu residues, which is inactive with respect to coagulation, is released into the bloodstream.[1] Prothrombin in this form is called des-gamma-carboxy prothrombin (DCP) or protein induced by vitamin K absence/antagonist-II (PIVKA-II). As the number of Glu residues unconverted to Gla varies, DCP is present as a mixture of prothrombin with various numbers of Glu residues, ranging from 1 to 10. In addition, because the Gla residue can bind to calcium, it is known that the 3-D protein structure of DCP will be different in the presence of calcium, and depends on the number of Glu residues.[2]

Des-gamma-carboxy prothrombin is frequently found in the blood of patients with hepatocellular carcinoma (HCC). Because DCP is elevated in many patients with HCC but not in patients with chronic hepatitis or cirrhosis without HCC,[3] it has been routinely used as a tumor marker of HCC in clinical settings.[4–6] However, serum DCP levels are also increased in the absence of HCC when there is a shortage of vitamin K or in the presence of vitamin K antagonists.[7] The value of DCP as a marker of HCC, therefore, is significantly reduced in patients who are taking vitamin K antagonists such as warfarin.

Previous studies reported differences in the number of Glu residues in DCP between patients with HCC and patients taking vitamin K antagonists.[8,9] Conventionally, DCP is measured using a mAb produced by the cell line MU-3 (Picolumi PIVKA-II; EIDIA, Tokyo, Japan), which reportedly reacts predominantly with DCP with 9–10 Glu residues. MU-3 had lower affinity for DCP with one to five Glu residues.[10] However, measuring DCP with this antibody alone can not differentiate between HCC-induced and vitamin K antagonist-associated elevations of DCP, making it difficult to evaluate whether rises in DCP are caused by HCC in patients taking vitamin K antagonists.

In the present study, we attempted to identify HCC-induced DCP in patients with HCC taking the vitamin K antagonist warfarin through the use of two mAbs against DCP, P-11 and P-16 (Sekisui Medical, Tokyo, Japan), which have a reactivity profile different from MU-3. We found clinical utility in DCP as a marker for HCC in patients taking warfarin when measured with the combination of MU-3, P-11, and P-16.

Materials and Methods

Preparation of electrochemiluminescence immunoassay (ECLIA) reagents with P-11 and P-16. Magnetic beads coated with P-16 mAb (Sekisui Medical) were prepared as follows: 1 mL of 30 mg/mL magnetic bead suspension (Dynabeads M-450 Epoxy; Life Technologies, Carlsbad, CA, USA) was placed into a test tube and the magnetic beads were trapped by a magnet to separate the supernatant. After the supernatant was discarded, 1 mL P-16 mAb (0.5 mg/mL in 0.15 mol/L PBS, pH 7.8) was added to the magnetic beads and stirred at 25°C for 18 h. After washing the magnetic beads, 2 mL of 1% BSA in 0.15 mol/L PBS (pH 7.8) were added and stirred at 25°C for 18 h to block the beads. These beads were diluted to 1 mg/mL using the bead dilution reagent (0.05 mol/L Tris buffer (pH 7.5), 0.15 mol/L NaCl, 0.01% Tween 20, 0.1% NaN_3, 10% normal rabbit serum, and 0.1% mouse serum) when in use.

Ruthenium (Ru)-conjugated P-11 mAb was prepared by the following procedure: 68 μL Ru-complex compounds (10 mg Ru (II) Tris (bipyridyl)-NHS ester in 1 mL DMSO) was added

[4]To whom correspondence should be addressed.
E-mail: tkumada@he.mirai.ne.jp

doi: 10.1111/j.1349-7006.2012.02232.x

to 1 mL P-11 mAb (1 mg/mL in 0.15 mol/L PBS, pH 7.8) (Sekisui Medical) for conjugation, and stirred at 25°C for 30 min. Then, 50 μL of 2 mol/L glycine was added to terminate the conjugation reaction, and Ru-conjugated P-11 mAb was isolated by collecting the Ru-bound protein fraction using Sephadex G-25 (previously equilibrated with 10 mmol/L PBS, pH 6.0). The Ru-conjugated P-11 mAb was then diluted to 1 μg/mL using Ru dilution reagent (0.015 mol/L HEPES buffering solution [pH 7.8], 0.15 mol/L NaCl, 0.013 mol/L $CaCl_2$, 0.1% Tween 20, 0.1% NaN_3, 5% normal rabbit serum, and 0.1% mouse serum) when in use.

Measurement of conventional DCP (with MU-3 antibody), NX-DCP (with P-11 and P-16 antibodies), and NX-DCP ratio. Conventional DCP, which is measured using MU-3 antibody and is currently used in clinical settings, was measured with ECLIA using the Picolumi III automated analyzer (EIDIA). NX-DCP was measured by ECLIA. Briefly, 25 μL magnetic beads coated with P-16 mAb (1 mg/mL) and 150 μL Ru-conjugated P-11 mAb (1 μg/mL) were added to samples at 30°C for 9 min to obtain the value of NX-DCP. The NX-DCP ratio was calculated by dividing the value of DCP measured using the conventional Picolumi method by the value of NX-DCP.

Reactivity of MU-3, P-11, and P-16 mAbs based on the time allowed for decarboxylation from prothrombin. We prepared DCP with varying numbers of Glu residues by applying different time intervals for decarboxylation from prothrombin (Enzyme Research Laboratories, Swansea, UK), according to the method of Bajah *et al.*[2] Specifically, 0.78 mL ammonium bicarbonate solution (0.1 mol/L, pH 8.0) was applied to 4.6 mg/mL prothrombin solution overnight for dialysis against an ammonium bicarbonate solution at 4°C. Then 0.1 mol/L EDTA*2Na was applied to the solution after dialysis until a final concentration of 10 mmol/L was achieved, and the solution was allowed to stand at room temperature for 30 min. This solution was dialyzed again against an ammonium bicarbonate solution for 2 h at 4°C then aliquoted into six heat-resistant vials with a screw cap and lyophilized. The vials were then filled with nitrogen gas and heated to 110°C for 0, 30 min, 1, 2, 6, or 23 h to create six different samples. We coated microplates with 100 μL of each sample at 0.1 μg/mL, and tested reactivity of the MU-3, P-11, and P-16 mAbs in the presence of 4 mmol/L calcium chloride. The experiments were repeated three times and the average value was calculated.

Patients. A total of 338 patients were diagnosed with primary, non-recurrent HCC between January 2006 and December 2009 at Ogaki Municipal Hospital (Ogaki, Japan). Of these, 14 patients had been taking warfarin when HCC was diagnosed. Six patients at Osaka Red Cross Hospital (Osaka, Japan) who were diagnosed as having primary HCC during the same period and had been taking warfarin at the time of diagnosis were also enrolled in the study. We analyzed the stored serum samples from these 20 patients, obtained at the time of HCC diagnosis. The diagnosis of HCC was made by histological examination or appropriate imaging characteristics using criteria of the guidelines by the American Association for the Study of Liver Diseases.[1] Tumor stage on imaging findings was assessed according to the TNM classification of the Liver Cancer Study Group of Japan.[12]

Control samples were obtained from 56 patients with chronic liver disease without HCC who were followed up at Ogaki Municipal Hospital. Samples were collected during routine HCC surveillance during the same period. These patients had been taking warfarin when serum samples were collected and provided informed consent for their stored serum samples to be used for research. The diagnosis of chronic liver disease was made with histological examination in 45 patients, including 10 with cirrhosis. The remaining 11 patients were diagnosed with cirrhosis based on imaging findings and biochemical tests. To ensure that controls did not have HCC, these patients were followed for 3 years after serum sampling by ultrasonography, CT, or MRI to ensure that none had developed HCC.

The protocol for the clinical part of this study was approved by the institutional review board of Ogaki Municipal Hospital and carried out in compliance with the Helsinki Declaration. Written informed consent was obtained from all study patients for the use of clinical and laboratory data and stored serum samples.

Statistical analyses. Differences in percentages between groups were analyzed using the χ^2-test. Differences in mean quantitative values were analyzed by the Mann–Whitney *U*-test. Changes in the NX-DCP ratio with increases in HCC stage were analyzed with the Jonckheere–Terpstra test. Data analyses were carried out using JMP statistical software, version 6.0 (Macintosh version; SAS Institute, Cary, NC, USA). All *P*-values were derived from two-tailed tests, with $P < 0.05$ considered to indicate statistical significance.

Results

Reactivity of MU-3, P-11, and P-16 antibodies with DCP based on time allowed for decarboxylation from prothrombin. Figure 1 shows the reactivity of the MU-3, P-11, and P-16 antibodies according to the time allowed for decarboxylation from prothrombin. MU-3 did not react with prothrombin (0 min) and its reactivity increased as the heating time (time allowed for decarboxylation) increased, with maximum reactivity to the sample after 6 h of heating. In contrast, P-11 and P-16 showed maximum reactivity to the 1-h sample and reactivity decreased as the heating time (time allowed for decarboxylation) increased.

Patient characteristics and levels of conventional DCP, NX-DCP, and NX-DCP ratio. Warfarin was used to treat atrial fibrillation in 48 patients, a history of mitral or aortic valve replacement in 13 patients, and a history of cerebral infarction in 15 patients. Table 1 summarizes the characteristics of the patients with and without HCC. There were no differences in patient

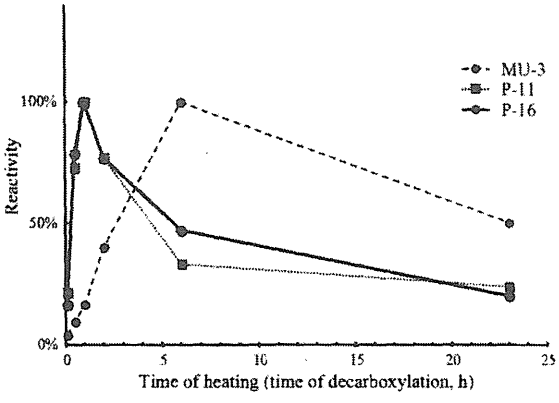

Fig. 1. Reactivity of MU-3, P-11, and P-16 antibodies according to the time allowed for decarboxylation from prothrombin. MU-3 did not react with prothrombin (0 min) and its reactivity increased as the heating time (time allowed for decarboxylation) increased, with maximum reactivity to the sample after 6 h of heating. Both P-11 and P-16 showed maximum reactivity to the 1-h sample and reactivity decreased as the heating time increased.

doi: 10.1111/j.1349-7006.2012.02232.x

Table 1. Background characteristics of study patients with and without hepatocellular carcinoma (HCC) (n = 76)

	Patients with HCC (n = 20)	Patients without HCC (n = 56)	P-value
Mean age ± SD, years (range)	72.4 ± 8.0 (46–83)	70.0 ± 9.8 (46–86)	0.3211
Sex, female/male	6 (30.0)/14 (70.0)	19 (33.9)/37 (66.1)	0.9651
Albumin, g/dL (mean ± SD)	3.82 ± 0.42	3.97 ± 0.51	0.2276
Total bilirubin, mg/dL (mean ± SD)	1.02 ± 0.65	0.82 ± 0.52	0.1288
Platelets ($\times 10^3/\mu L$)	158 ± 75	160 ± 49	0.4754
INR	1.75 ± 0.58	1.76 ± 0.58	0.7816
Mean tumor size ± SD, cm (range)	3.35 ± 1.84 (1.1–8.4)	–	–
Number of tumors, single/multiple	15 (75.0)/5 (25.0)	–	–
Tumor stage, I/II/III†	3 (15.0)/11 (55.0)/6 (30.0)	–	–

†According to the TNM classification of the Liver Cancer Study Group of Japan. Unless otherwise indicated, values in parentheses indicate percentages. INR, International normalized ratio.

age, sex, serum albumin, serum total bilirubin, platelet count, or prothrombin levels.

Figure 2 compares conventional DCP levels, NX-DCP levels, and NX-DCP ratios between patients with and without HCC. No differences were found in conventional DCP levels between patients with and without HCC (median, 2600.5 mAU/mL and range, 1060–96920 mAU/mL in patients with HCC versus median, 20550.5 mAU/mL and range, 1355–71783 mAU/mL in patients without HCC; P = 0.7952). In contrast, NX-DCP levels in patients with HCC (median, 34135.0 mAU/mL; range, 260–67581 mAU/mL) were significantly lower than in patients without HCC (median, 40708.0 mAU/mL; range, 5026–60443 mAU/mL; P = 0.0291). As a result, the NX-DCP ratio was significantly higher in patients with HCC (median, 1.92; range, 0.35–10.32) than in patients without HCC (median, 0.49; range, 0.12–1.33; $P < 0.0001$).

Sensitivity, specificity, and positive and negative predictive values of NX-DCP ratio for diagnosis of HCC. Figure 3(a) shows the receiver operating characteristic (ROC) curve of the NX-DCP ratio for the diagnosis of HCC. The area under the ROC curve was 0.8928. The highest Youden index was 0.68 when the cut-off was fixed as 0.65 and the highest accuracy was 89.5% when the cut-off was fixed as 1.50, based on the sensitivity and specificity analysis (Fig. 3b). When the cut-off was fixed as 0.65, sensitivity, specificity, positive predictive value (PPV), negative predictive value (NPV), and accuracy were 95.0%, 73.2%, 55.9%, 97.6%, and 78.9%, respectively. When the cut-off was fixed as 1.50, sensitivity, specificity, PPV, NPV, and accuracy were 60.0%, 100.0%, 100.0%, 87.5%, and 89.5%, respectively.

Serum alpha-fetoprotein (AFP) and *Lens culinaris* agglutinin-reactive fraction of AFP (AFP-L3) levels in patients with HCC. Serum levels of AFP and AFP-L3 were measured[13] in patients with HCC in the same serum for the measurement of NX-DCP ratio (AFP-L3 was not measured in five patients). The median (range) values were 18.4 ng/mL (0.8–68 470 ng/mL) for AFP and 3.6% (0–45.2%) for AFP-L3. When the cut-off levels of AFP and AFP-L3 were fixed as 20 ng/mL and 5%, respectively, according to previous reports,[14–16] 10 of 20 patients (50.0%) showed elevation of AFP and seven of 15 patients (46.7%) showed elevation of AFP-L3. These two tumor markers were not increased in six of 15 patients (40.0%).

NX-DCP ratio and progression of HCC. Figure 4 shows the NX-DCP ratio in patients according to HCC stage. Despite the small number of patients, there was a gradual increase in the NX-DCP ratio as the stage increased (P = 0.0315).

Discussion

Hepatocellular carcinoma is the sixth most common cancer and the third most common cause of cancer-related death worldwide.[17,18] In Japan, HCC is currently the third most common cause of death from cancer in men and the fifth in women.[19] The incidence of HCC is also increasing in the US.[20,21] Improvements of tumor markers specific for HCC contribute to early detection of HCC. Three markers for HCC are currently used clinically, AFP, AFP-L3, and DCP. The utility of each of these tumor markers for detection and diagnosis of HCC, for evaluation of tumor progression, and for determination of patient prognosis has been reported.[4,22–24] Elevation

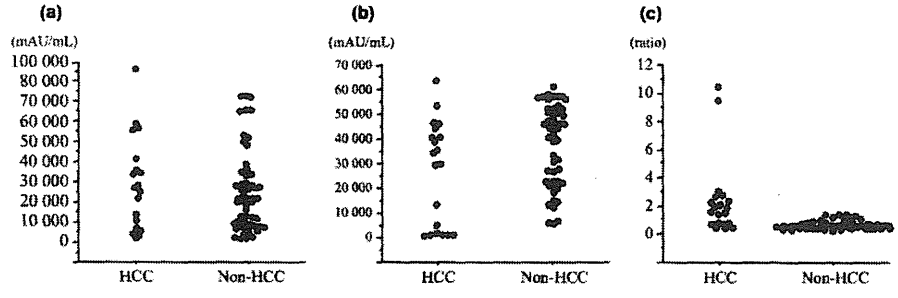

Fig. 2. Serum levels of conventional des-gamma-carboxy prothrombin (DCP), NX-DCP, and the NX-DCP ratio in patients with and without hepatocellular carcinoma (HCC) taking warfarin. (a) Serum levels of conventional DCP. No differences were found between two groups (P = 0.7952). (b) Serum levels of NX-DCP were significantly higher in patients without HCC compared to those with HCC (P = 0.0291). (c) The NX-DCP ratio was significantly higher in patients with HCC than in those without HCC, consequently ($P < 0.0001$).

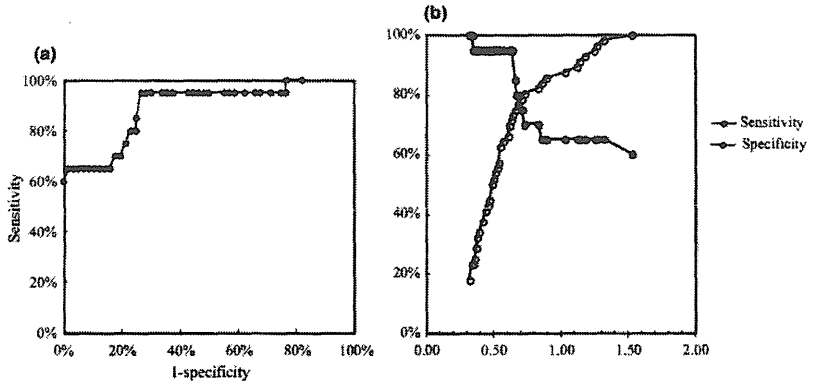

Fig. 3. Receiver operating characteristic (ROC) analysis and the determination of cut-off level of the NX-DCP ratio for the diagnosis of hepatocellular carcinoma. (a) The area under the ROC curve was 0.8928. (b) The highest Youden index was 0.68 when the cut-off was fixed as 0.65 and the highest accuracy was 89.5% when the cut-off was fixed as 1.50.

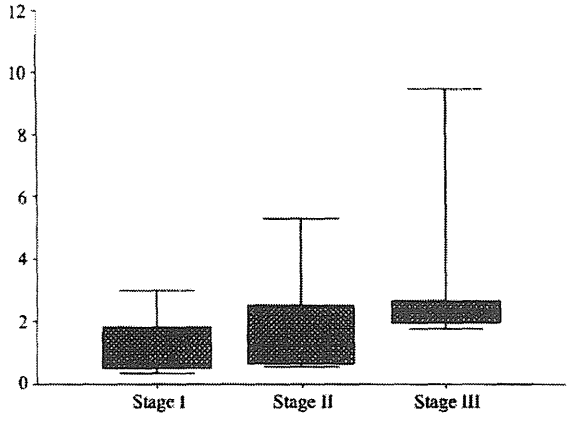

Fig. 4. The NX-DCP ratio according to hepatocellular carcinoma (HCC) stage in 20 patients with HCC taking warfarin (box plot). There was a gradual increase in the NX-DCP ratio as the HCC stage increased ($P = 0.0315$).

of DCP is often observed in HCC patients without elevation of AFP or AFP-L3, and is useful as a complement to these other two markers in the diagnosis of HCC. In addition, elevation of DCP is reportedly associated with a high rate of portal vein invasion and poor prognosis.[25] Elevation of DCP is also associated with better outcomes when hepatectomy, rather than radiofrequency ablation, is carried out in patients treated with curative intent.[26,27]

However, DCP loses its value as a tumor marker of HCC in patients taking warfarin.[7] Due to the marked decrease in vitamin K level caused by warfarin intake, DCP levels significantly increase in individuals taking warfarin, even in the absence of HCC. Therefore, DCP has no clinical utility as a tumor marker for HCC in this patient subpopulation.

The present study evaluated the reactivity of new antibodies against DCP, antibodies P-11 and P-16, based on the number of Glu residues. The number of Glu residues increases as the time allowed for decarboxylation from prothrombin increases.[2] Our results showed P-11 and P-16 have higher reactivity with DCP with fewer Glu residues than MU-3, the antibody that is conventionally used for the measurement of DCP. The NX-DCP level that is measured by P-11 and P-16 antibodies, therefore, represents predominantly DCP caused by reduced vitamin K availability. Consequently, the elevation of the NX-DCP ratio calculated in the equation: conventional DCP/NX-DCP, reflects more specifically the elevation of DCP by HCC.

There were no differences in the conventional measurements of DCP between patients with and without HCC who are taking warfarin. The NX-DCP ratio was significantly lower in patients without HCC than in patients with HCC. The NX-DCP ratio varied in patients with HCC, as was conventional DCP in patients not taking warfarin, because the production of DCP by HCC is variable. In contrast, in all patients without HCC, the NX-DCP ratio was low despite high conventional DCP levels in the same patients; no patients had an elevated NX-DCP ratio. The results indicate that the NX-DCP ratio could pinpoint the elevation of DCP caused by HCC, thereby restoring the value of DCP as a marker for HCC in patients taking warfarin.

When the cut-off level was fixed at 1.5 on the basis of maximal accuracy, the sensitivity, specificity, PPV, and NPV were comparable to those of conventional DCP in the general population with normal vitamin K levels, as previously reported.[28] The NX-DCP ratio, therefore, seems to be useful as a marker for HCC in patients taking warfarin.

The elevation of other tumor markers for HCC, AFP and AFP-L3, were observed in only half of the patients with HCC taking warfarin. In addition, both AFP and AFP-L3 were negative in 40% of patients with HCC. Des-gamma-carboxy prothrombin is a complimentary marker of AFP/AFP-L3 for HCC. The elevation of DCP without the elevation of AFP and AFP-L3 was observed in 16.1% of patients (cut-off, 20 ng/mL for AFP, 10% for AFP-L3, and 40 mAU/mL for DCP)[29] and 24.8% of patients (cut-off, 400 ng/mL for AFP, 15% for AFP-L3, and 100 mAU/mL for DCP).[30] The measurement of the NX-DCP ratio, therefore, will be important for the detection and diagnosis of HCC even when AFP or AFP-L3 is measured simultaneously.

There are several limitations to this study. The most important limitation was the small number of study patients, especially patients with HCC. The number of patients with HCC taking warfarin is low, so it was difficult to increase the number of study patients. Consequently, it was difficult to evaluate the value of the NX-DCP ratio in indicating progression of

doi: 10.1111/j.1349-7006.2012.02232.x